INORGANIC MATERIALS
AND NANOMATERIALS

Recovery of Sb³⁺ Ions by Biogenic Silicon-Containing Materials

A. N. Kholomeidik[a], * and **A. E. Panasenko[a]**

[a] *Institute of Chemistry, Far Eastern Branch, Russian Academy of Sciences, Vladivostok, 690002 Russia*
*e-mail: anik@ich.dvo.ru

Abstract—Functional silicon-containing materials—silicon—carbon product, high-purity amorphous silicon dioxide, sodium aluminosilicate, and iron-containing magnetoactive composite material with specific surface area from 56.7 to 470 m²/g—have been obtained from agricultural wastes (rice husk and straw). Chemical and phase composition of obtained samples have been determined, particle morphology has been established by scanning electron microscopy, specific surface area has been measured, IR spectra have been recorded. The possibility to use the obtained materials for the removal of antimony ions from aqueous solutions has been studied. It has been found that sodium aluminosilicate and iron-containing composite materials based on biogenic silica show high capacity toward antimony ions: 596 and 386 mg/g, respectively. Used approach, in the first place, allows one to reclaim safely rice straw and husk and to reduce atmospheric emission of microdisperse amorphous silica SiO_2 resulting from their open combustion and causing respiratory diseases. In the second place, the study enables purification of natural and technogeneous wastewaters contaminated by antimony(III), which form on the sites of antimony rock deposits on their decay and mining.

Keywords: rice production wastes, biogenic silica, aluminosilicates, iron-containing composites, antimony(III)

DOI: 10.1134/S0036023622090066

INTRODUCTION

Antimony compounds occur in nature due to natural processes (ablation of rocks, volcanic activity) and anthropogenic impact [1]. Antimony and its compounds are used in production of ceramics, accumulators, fire retardants, catalysts, and pigments [2]. The world stock of antimony is more than 2 million tons; it is located in Bolivia, China, Russia, South Africa, and Mexico [3]. The most acute problem of environment contamination by antimony is observed in the regions of its extraction from deposits, in particular, elevated antimony content in ground and surface waters (up to 6.38 mg/L [4], at permitted Sb content of in water of 0.005 mg/L (Sanitary Regulations and Standards 1.2.3685−21)) is observed in China, which remains to be leader in antimony production according to the report of the United States Geological Survey for 2021, China extracts more than 52% of world ore output [5].

Excess antimony content in environment is known to result in death of animals, soil organisms and bacteria and causes diseases of hemopoietic, cardiovascular, and respiratory systems of human [6]. Therefore, it is urgent task to recover antimony ions from sewage, ground, and surface water.

Purification of sewage water from antimony is carried out by different methods including such as coagulation, flocculation [7], membrane method [8], ion exchange [9], and sorption [10]. Due to efficiency and low cost, sorption method of purification is the most widespread. Materials of mineral origin are used as sorbents most frequently [6, 11], the highest parameters are observed for materials containing silicon and/or iron [12]. Modified silicas are widely used for the sorption of different pollutants [13].

Rice production wastes—husk and straw—are widely used in different industry areas to obtain silicon-containing materials, high-purity silica including [14, 15]. Silica, silicates, aluminosilicates, and composite materials of biogenic origin are of interest as sorption-active materials because, in contrast to mineral analogs, they have constant composition and contain noticeably less admixtures of foreign elements.

On the other hand, there is a problem of disposal of agricultural waste of rice manufacture. Rice straw and husk are preferably turned under fields or incinerated [16]. However, these methods are unsatisfactory from environmental viewpoint because of low rate of biodegradation and evolution of silica microparticles on incineration, which cause lung diseases in the regions of rice production [17]. The use of rice straw and husk as a source of silicon and raw materials for the synthesis of silicate materials allows one to solve environmental problem of agricultural waste disposal.

In this work, we obtained silicon-containing oxide materials of different composition from rice husk and

Table 1. Characteristics of samples

Sample	Raw material	Composition, %	S_{sp}, m^2/g	pH of aqueous suspension	A^*, mg/g
1	Rice husk	SiO$_2$, 53.9; C, 39.1	300	5.5	6.1
2	Rice husk	SiO$_2$, 99.9	295	6.5	13.7
3	Rice straw	SiO$_2$, 51.1; Al$_2$O$_3$, 39.8; Na$_2$O, 13.5	470	7.0	596
4	Rice husk	SiO$_2$, 92.5; Fe$_2$O$_3$, 3.1	56.7	7.0	386

*A is capacity of material toward antimony(III) ions.

straw and studied the possibility to use these materials for recovery of antimony ions from aqueous solutions.

EXPERIMENTAL

As a subject of study, we used silicon-containing materials obtained by different methods from rice husk and straw. Sample 1: rice husk was exposed to two-stage calcinations at 300 and 500°C similarly to [18]. Sample 2: rice husk was treated with 0.1 M hydrochloric acid solution at 90°C for 1 h, filtered off, washed with water, dried, and calcined at 600°C similarly to [19]. Sample 3: rice straw was treated with 0.1 M NaOH solution (ratio s : l = 1 : 13) at 90°C for 1 h. The resultant hydrolysate was separated by filtration from solid cellulose residue, diluted aqueous solution of aluminum sulfate was added, and the solution was adjusted to pH 7. The resultant precipitate was separated by decantation, washed, and dried at 105°C similarly to [20]. Sample 4: amorphous silicon dioxide (sample 2) was impregnated with 6% aqueous solution of iron(III) oxalate followed by calcination at 400°C similarly to [21, 22].

Elemental analysis was performed by energy dispersive X-ray fluorescent spectroscopy on a Shimadzu EDX 800 HS spectrometer (Japan). IR absorption spectra in the range 400–4000 cm^{-1} were registered in Nujol mull on a Bruker Vertex 70 (Germany) Fourier-transform spectrometer. X-ray diffractograms were recorded on a Bruker D8 Advance (Germany) diffractometer in CuK_α radiation. Phases were identified by EVA software using PDF-2 database. Micrographs were obtained on a Hitachi S-5500 (Japan) and a Thermo Scientific Phenom ProX (USA) scanning electron microscopes. Value of aqueous suspension pH was determined at ratio s : l = 1 : 10 according to [23] on a Hanna Edge HI2020 (USA) pH-meter. Specific surface area of samples (S_{sp}, m^2/g) was determined by the standard procedure [24] by the formula:

$$S_{sp} = A_{max} 6.022 \omega_0,$$

where A_{max} is a capacity of monolayer of adsorbed Methylene Blue, mmol/g,

ω_0 is the area occupied by a molecule of adsorbed Methylene Blue in a dense monolayer on the surface of sample.

Experiment on the recovery of Sb^{3+} ions was conducted under static conditions from aqueous solutions of SbF$_3$ and NaSbF$_4$ with metal concentration of 20–1000 mg/L at ratio of solid and liquid phases (s : l) of 1 : 1000 at ambient temperature. Solution pH was not corrected during experiment.

Antimony ions concentration in solution was determined by atomic absorption spectrometry on a Nippon Jarrell Ash AA-770 (Japan) spectrophotometer in acetylene–air flame.

One of parameters that determine material efficiency for antimony recovery is the capacity (A, mg/g), which was calculated by the formula:

$$A = \frac{(C_{ini} - C_{eq})}{m \times 1000} V,$$

where C_{ini} and C_{eq} are initial and equilibrium concentrations (mg/mL); V is solution volume (mL); m is weight of sample (g).

RESULTS AND DISCUSSION

Chemical composition and properties of samples are presented in Table 1. In spite of the use of rice production wastes as precursor, different schemes allow preparation of a number of materials different in composition and properties, including high-purity amorphous silica (99.9% SiO$_2$), silicon–carbon product (containing SiO$_2$ and C), sodium aluminosilicate, and iron-containing composite.

The obtained samples are X-ray amorphous as evidenced by diffuse maximum on X-ray diffractograms of samples in the region 22°–27° (Fig. 1). The magnitude of specific surface area varies in the range 56.7–470 m^2/g, sodium aluminosilicate (sample 3) has the largest specific surface area.

The IR spectra of amorphous silica obtained from rice husk by thermal treatment (sample 1) and by thermal treatment after acid hydrolysis (sample 2) according to [25] are similar to each other (Fig. 2, curve *a*). The data in Fig. 2 show that the spectra of samples studied in this work are similar to each other and contain absorption bands in the region 3385–3381 and 1641–1639 cm^{-1} corresponding to the deformational and stretching vibrations of water OH groups. Moreover,
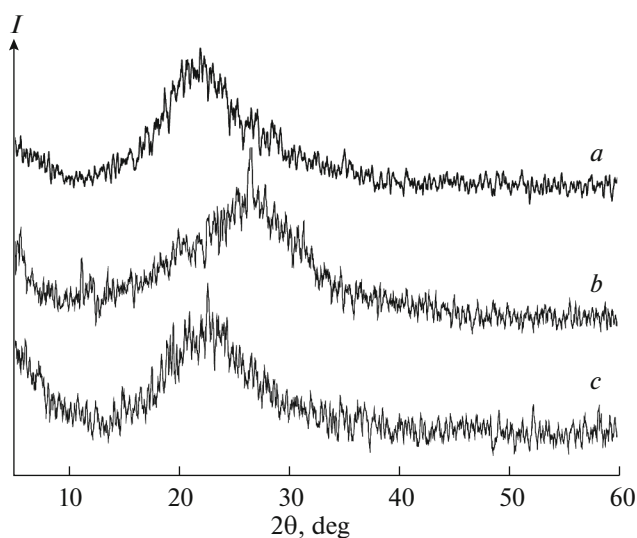
Fig. 1. X-ray diffraction patterns for samples: (*a*) 1, 2; (*b*) 3 (*c*) 4 (numbering corresponds to Table 1).

IR spectra show absorption bands in the region 467–461, 800–797, and 1099–1014 cm^{-1} corresponding to the deformational and stretching (symmetrical and asymmetrical vibrations of siloxane bonds Si–O. The spectrum of iron-containing composite material (sample 4) displays bands in the region 952 cm^{-1}, which indicates the presence of silanol groups Si–OH (Fig. 2, curve *c*). The feature of spectrum of sample 3

(Fig. 2, curve *b*) is the presence of band typical for aluminosilicates in the region 700 cm^{-1} related to vibrations of Al–O–Si bond and the position of absorption band at 1014 cm^{-1} corresponding to the asymmetric stretching vibrations of Si–O bond.

The structure of the obtained samples is governed by preparation method and structure of biogenic silica, which in turn is dependent on the cell structure of vegetable tissues of rice husk and straw. The results of study presented in micrographs (Fig. 3) indicate that silicon–carbon material (sample 1) retains the structure of vegetable tissue, the surface of its particles is formed by the rows of cones connected to each other (Fig. 3a). The particles of pure amorphous silica (sample 2) also retain to some extent the structure of vegetable tissues, but they are more fragmentary (Fig. 3b). Aluminosilicate particles (sample 3) have disordered structure, extended surface, and complex system of pores about 0.5 μm in diameter, which causes high specific surface area of this sample (Fig. 3c). Sample 4 (Fig. 3d) consists of particles as globules of 55–80 in size, each of which includes several iron-containing nuclei 5–15 nm in size dispersed in silicon dioxide matrix.

To assess the possibility to recover antimony compounds by the studied samples, we draw the curves of Sb³⁺ ions recovery from aqueous SbF$_3$ solutions at metal concentration of 20–1000 mg/L under static conditions (Fig. 4a).
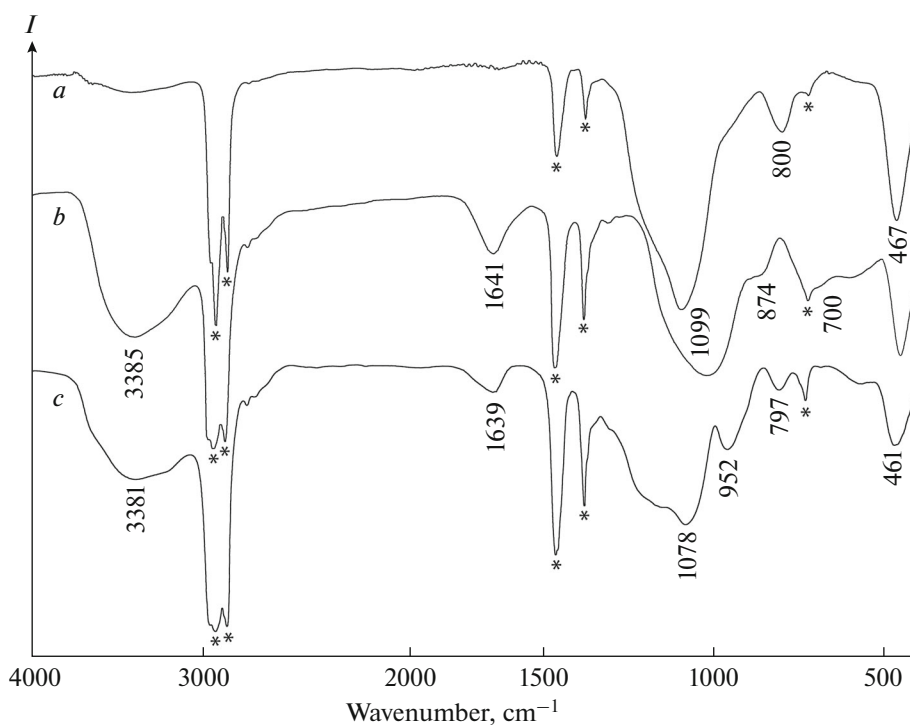

Fig. 2. IR spectra of samples: (*a*) 1, 2; (*b*) 3 (*c*) 4; asterisk * designates absorption bands of Nujol.
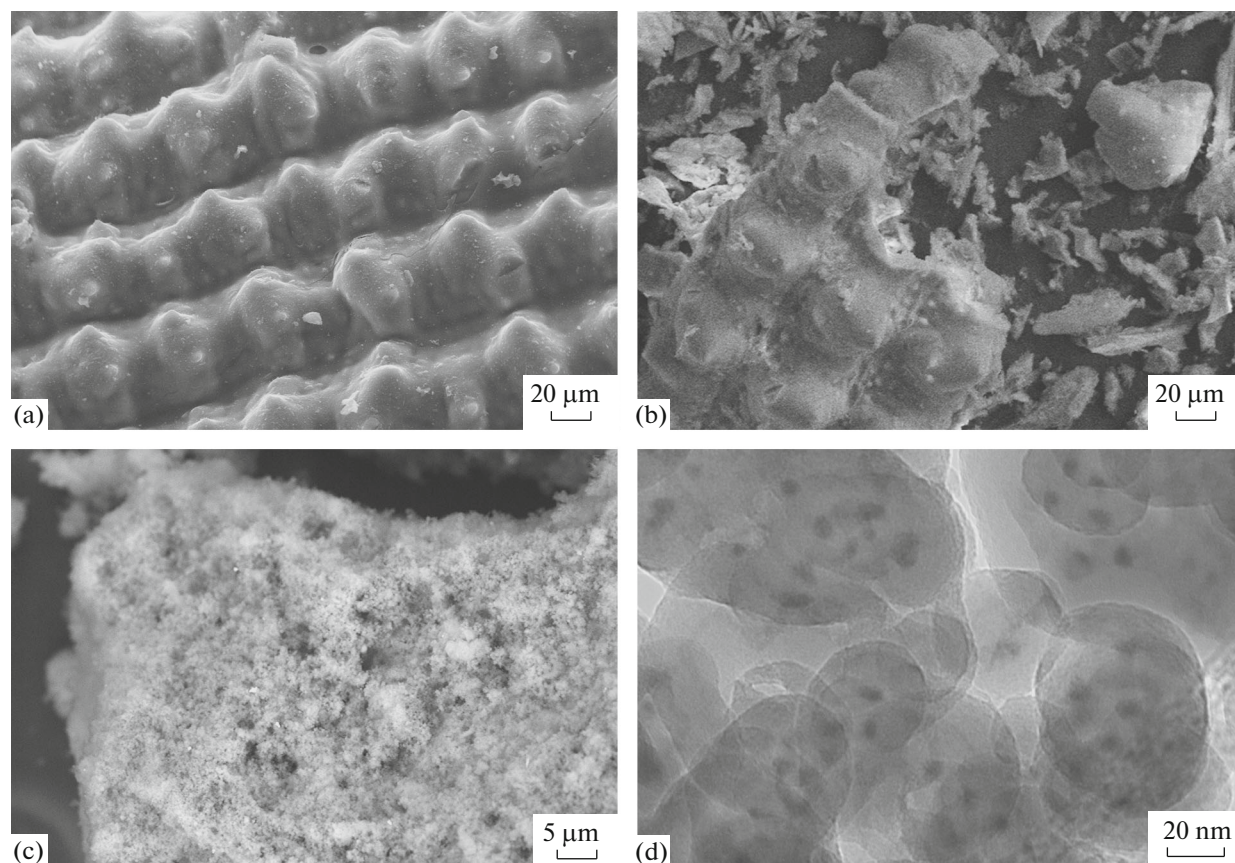
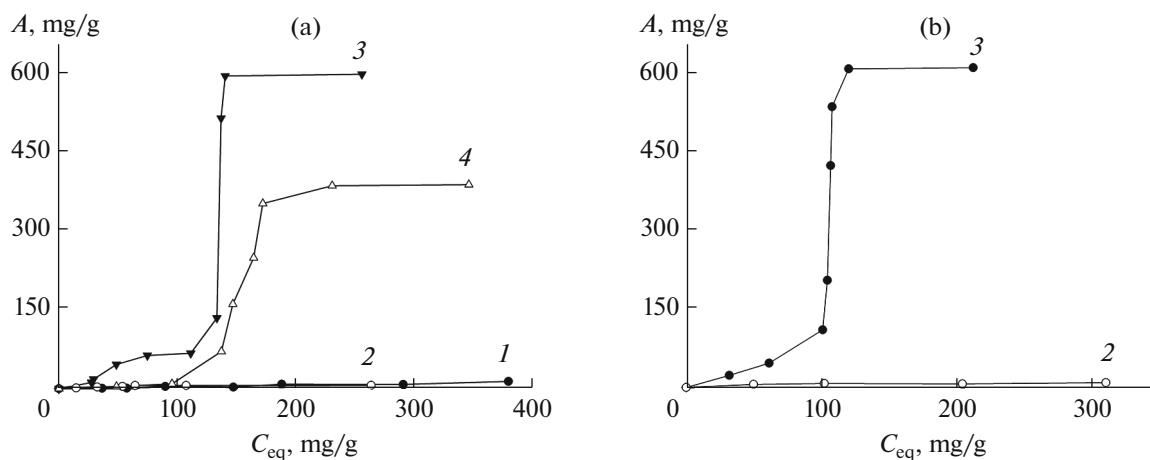**Fig. 3.** Micrographs of silicon-containing samples: (a) 1, (b) 2, (c) 3, (d) 4.

Fig. 4. Curves for Sb^{3+} recovery by silicon-containing samples $1-4$: (a) from SbF_3 solution; (b) from $NaSbF_4$ solution. C_{eq}, mg/mL is equilibrium concentration of antimony ions; A, mg/g is capacity.

The analysis of curves shown in Fig. 4a indicates that sodium aluminosilicate (sample 3) obtained from rice straw is the most efficient, its capacity is 596 mg/g. Among the known sorbents for antimony recovery in the studied concentration range, the majority displays sorption capacity about $100-250$ mg/g, and the best known material, birnessite, exhibits capacity of 759 mg/g [12]. The samples of silicon dioxide isolated by different methods from rice husk, both high-purity (sample 2) and carbon-containing (sample 1), show the least

capacity toward antimony ions. Iron-containing composite material (sample 4) prepared from high-purity amorphous silica (sample 2) is more efficient as compared to them. The capacity of this sample is 386 mg/g and exceeds by factor 1.5–2 the values of maximal capacity for argillaceous iron-containing materials of mineral origin studied in [6]. Possibly, due to paramagnetic properties [21], such materials can be used for the treatment of oncological diseases by target local delivery [26, 27] with the aid of magnetic field of antimony fluoride compounds showing antitumor properties [28].

Issue has been studied on how reaction of Sb(III) ions with material surface depends on the type of antimony compound in solution. The presence of such complexing agents as tartrate and citrate anions and EDTA is known to affect the extent of antimony recovery [29]. Different antimony(III) fluoride compounds form different stable complex anions in solutions [30]. To assess the effect of forms of antimony ions in solution, we conducted experiment similar to that described above on the recovery of Sb from $NaSbF_4$ solution. For this purpose, we used silicon dioxide (sample 1) and sodium aluminosilicate (sample 3), which showed the least and the maximal capacity, respectively. Recovery curves (Fig. 4) display that the recovery of Sb^{3+} ions from SbF_3 and $NaSbF_4$ solutions under studied conditions has the same character.

The difference in capacity for materials of different composition by two orders of magnitude is related to the nature of sample surface. So, the aqueous extracts of silicon–carbon material and silicon dioxide (samples 1 and 2) have weakly acidic pH (Table 1), while the aqueous suspensions of aluminosilicate and iron-containing composite material have neutral pH. Because fluoride solutions of antimony complexes have acidic pH [30], its recovery proceeds more efficiently on materials showing neutral or weakly alkaline medium, which is confirmed by experimental data. It is important to note that there is no correlation between specific surface area and capacity of the studied samples.

Based on the character of curves (Fig. 4a), antimony recovery from aqueous solutions on samples 3 and 4 proceeds by mixed mechanism, in spite of the fact that many literature sources [12] describe such recovery as a sorption. In the region of low concentrations, the main processes are the sorption of Sb^{3+} ions on the surface of the studied materials and cation exchange [31]. Recovery sharply increases with concentration. The reason of this feature in the case of sodium aluminosilicate is the hydrolysis of antimony on the surface of the material, which is confirmed by the data on hydrolysis of antimony fluorides in aqueous solutions [30]. In the case of iron-containing composite, recovery increases due to chemosorption process, which agrees well with the wide use of iron oxides

as highly-efficient materilas for water purification from antimony [6].

CONCLUSIONS

We obtained silicon-containing materials with specific surface area of 56.7–470 m^2/g from rice production wastes (straw and husk) by different methods of thermal and chemical treatment. We studied the ability of these materials to recover antimony aions from aqueous solutions. We have shown that silicon–carbon materials obtained by husk disposal by oxidizing roasting procedure are of little use for this purpose also like high-purity biogenic amorphous silica. Chemical synthesis with the use of rice straw as silicon source allows preparation of aluminosilicates showing high efficiency for antimony(III) recovery from aqueous solutions, which is close to the best known materials, the capacity of the studied samples of sodium aluminosilicate toward antimony reaches 596 mg/g. Iron-containing composite based on biogenic silica showing paramagnetic properties and suitable for magnetic separation and target delivery on exposure to external magnetic field also dispayed high capacity toward antimony (386 mg/g).

ACKNOWLEDGMENTS

FUNDING

CONFLICT OF INTEREST

The authors declare no conflicts of interest.

REFERENCES

1. M. He, N. Wang, and X. Long, J. Environ. Sci. **75**, 14 (2019).
   https://doi.org/10.1016/j.jes.2018.05.023

2. M. Filella, N. Belzile, and Y.-W. Chen, Earth-Sci. Rev. **57**, 125 (2002).
   https://doi.org/10.1016/S0012-825200070-8

3. W. C. Butterman and J. F. Carlin, *U.S. Geological Survey Mineral* (2004).
   https://doi.org/10.3133/ofr0319

4. X. Wang, M. He, J. Xi, et al., Microchem. J. **97**, 4 (2011).
   https://doi.org/10.1016/j.microc.2010.05.011

5. *Mineral Commodity Summaries. U.S. Geological Survey* (2021).
https://doi.org/10.3133/mcs2021

6. N. Wang, N. Deng, Y. Qiu, et al., Environ. Chem. **17**, 332 (2020).
https://doi.org/10.1071/EN20002

7. X. Guo, Z. Wu, and M. He, Water Res. **43**, 4327 (2009).
https://doi.org/10.1016/j.watres.2009.06.033

8. B. Ma, X. Wang, R. Liu, et al., J. Membr. Sci. **537**, 93 (2017).
https://doi.org/10.1016/j.memsci.2017.05.022

9. S. A. Awe and A. Sandstrom, Hydrometallurgy **137**, 60 (2013).
https://doi.org/10.1016/j.hydromet.2013.04.006

10. K. Yang, Y. Liu, Y. Li, et al., Chemosphere **232**, 254 (2019).
https://doi.org/10.1016/j.chemosphere.2019.124494

11. A. Anjum and M. Datta, J. Anal. Sci., Methods Instrument. **2**, 167 (2012).
https://doi.org/10.4236/jasmi.2012.23027

12. X. Zhang, N. Xie, Y. Guo, et al., J. Hazard. Mater. **418**, 126345 (2021).
https://doi.org/10.1016/j.jhazmat.2021.126345

13. G. V. Lisichkin and A. Y. Olenin, Russ. J. Gen. Chem. **91**, 870 (2021).
https://doi.org/10.1134/S1070363221050182

14. N. Soltani, A. Bahrami, M. I. Pech-Canul, et al., Chem. Eng. J. **264**, 899 (2015).
https://doi.org/10.1016/j.cej.2014.11.056

15. V. V. Samonin, E. A. Spiridonova, A. S. Zotov, et al., Russ. J. Gen Chem. **91**, 1546 (2021).
https://doi.org/10.1134/S107036322108017X

16. N. Ueasin, S-Y. Liao, and A. Wongchai, Energy Proc. **75**, 2757 (2015).
https://doi.org/10.1016/j.egypro.2015.07.518

17. S. Liu, N. Liu, and J. Li, J. Occupational Health **38**, 57 (1996).
https://doi.org/10.1539/joh.38.57

18. L. A. Zemnukhova, G. A. Fedorishcheva, A. G. Egorov, et al., Russ. J. Appl. Chem. **78**, 319 (319).
https://doi.org/10.1007/s11167-005-0283-2

19. A. G. Ladatko, L. A. Zemnukhova, G. A. Fedorishcheva, et al., Risovodstvo **7**, 100 (2005).

20. A. E. Panasenko, P. D. Borisova, O. D. Aref'eva, et al., Khim. Rastit. Syr. **3**, 291 (2019).
https://doi.org/10.14258/jcprm.2021017521

21. A. E. Panasenko, I. A. Tkachenko, A. A. Kvach, et al., Russ. J. Inorg. Chem. **62**, 971 (2017).
https://doi.org/10.1134/S0036023617070166

22. N. P. Shapkin, I. G. Khal'chenko, V. S. Pechnikov, et al., Russ. J. Inorg. Chem. **65**, 1614 (2020).
https://doi.org/10.1134/S0036023620100186

23. K. V. Ikonnikova, L. F. Ikonnikova, T. S. Minakova, et al., *Theory and Practice of pH-Metric Determination of Acid-Base Properties of the Surface of Solids* (Nats. Issled. Tomsk. Politekh. Univ., Tomsk, 2011) [in Russian].

24. N. V. Kel'tsev, *Fundamentals of Adsorption Technology* (Khimiya, Moscow, 1984) [in Russian].

25. L. A. Zemnukhova, A. E. Panasenko, E. A. Tsoi, et al., Inorg. Mater. **50**, 75 (2014).
https://doi.org/10.1134/S0020168514010208

26. B. A. Zasonska, A. Liskova, M. Kuricova, et al., Croatinmedical J. **57**, 165 (2016).
https://doi.org/10.3325/cmj.2016.57.165

27. S. Mourdikoudis, A. Kostopoulou, and A. P. LaGrow, Adv. Sci. **8**, 2004951 (2021).
https://doi.org/10.1002/advs.202004951

28. L. A. Zemnukhova, RF Patent 2298407, *Byull. Izobret.*, 2004, no. 13.

29. N. Bolan, M. Kumar, E. Singh, et al., Environ. Int. **158**, 106908 (2022).
https://doi.org/10.1016/j.envint.2021.106908

30. N. M. Laptash, E. V. Kovaleva, and A. Yu. Mashkovskii, J. Struct. Chem. **48**, 848 (2007).
https://doi.org/10.1007/s10947-007-0126-5

31. S. B. Yarusova, P. S. Gordienko, A. E. Panasenko, et al., Russ. J. Phys. Chem. **93**, 333 (2019).
https://doi.org/10.1134/S003602441902033

Translated by I. Kudryavtsev